Effect of the degradation of different dissolved NOM fractions by the heterogeneous Fenton treatment on the emergence of trihalomethanes and haloacetic acids at drinking water treatment plants

Omar J. Cotazo-Mosquera [a], Viviana A. Gómez-Obando [a], Luis-Alejandro Galeano [a], Ricardo A. Torres-Palma [b,*], Ana M. García-Mora [a,*,1]

[a] Grupo de Investigación en Materiales Funcionales y Catálisis (GIMFC), Departamento de Química, Universidad de Nariño, Calle 18, Cra. 50 Campus Torobajo, 520002 Pasto, Colombia
[b] Grupo de Investigación en Remediación Ambiental y Biocatálisis (GIRAB), Instituto de Química, Facultad de Ciencias Exactas y Naturales, Universidad de Antioquia UdeA, Calle 70 No. 52-21, 050010 Medellín, Colombia

ABSTRACT

Hydrophobic, hydrophilic, and transphilic fractions of natural organic matter, which are all present in drinking water treatment plants, can play a crucial role on the formation of disinfection by-products after chlorination. In this work, catalytic wet peroxide oxidation (heterogeneous-Fenton) activated by an aluminum/iron-pillared clay catalyst, was tested as an alternative to remove different organic fractions and evaluated its effect on disinfection by-products formation in several stages of two full-scale drinking water treatment plants in *Nariño* (Colombia). The advanced treatment removed 87 % hydrophobic, 36 % hydrophilic, and 70 % transphilic fractions in raw water with mostly hydrophobic character, while in the hydrophilic case, it was removed 47 % hydrophobic, and 40 % hydrophilic fractions. Interestingly, formation of trihalomethanes was reduced in up to 81 %, and haloacetic acids in up to 83 %. Also, the process significantly degraded high (~661 kDa) and low (~6.2 kDa) average molecular weight hydrophobic fractions into lighter, but less disinfection by-products forming ones. Meanwhile, the high average molecular weight (~1000 kDa) hydrophilic fraction was instead transformed into a lighter fraction (<3 kDa). The process showed to be highly efficient to degrade natural organic matter with different polar nature at room temperature and natural pH. However, the application of this treatment on the effluent of a conventional physicochemical unit (from hydrophilic water supply sources) must be avoided, since the residual organic content displayed higher potential for haloacetic acids formation. On the contrary, in hydrophobic water supply sources, it is recommended to apply the process at this point of treatment.

1. Introduction

Conventional water treatment methods, such as coagulation-flocculation, mainly reach the removal of the hydrophobic fraction of natural organic matter (NOM) exhibiting high molecular weights [1]. Therefore, the remaining hydrophilic and low molecular weight organics may produce significant amounts of disinfection by-products (DBP) such us trihalomethanes (THM) and haloacetic acids (HAA) upon chlorination [2]. THM and HAA have been regulated in several developing countries by different organizations. The United States Environmental Protection Agency imposes a maximum of 80 μg/L for

total THM and 60 μg/L for HAA_5 [3–5], while Health Canada allows 100 μg/L for total THM and 80 μg/L for HAA_5 [6,7], and the European Union 100 μg/L for total THM [8]. In Colombia, only total THM are regulated, and a maximum value 200 μg/L are permitted [9]; however, the policy does not clearly establish whether the monitoring and control of these substances should be done at the outlet of the drinking water treatment plant (DWTP) or in the water distribution system. The toxic effects of DBP are well known and it is currently an issue of particular concern, especially for drinking water in developing countries [10–12].
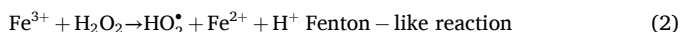
In recent years, advanced oxidation processes (AOP) have emerged as effective alternatives in the removal of residual NOM after conven-

tional treatment [13–18]. Among these, the heterogeneous Fenton processes [19] have been used to degrade NOM. In fact, the catalytic wet peroxide oxidation (CWPO), a heterogeneous Fenton system, could be a potentially cost-effective process, useful in drinking water applications, since it can operate under very mild conditions of temperature and pressure (ambient), and within a wider range of pH values than the conventional homogeneous Fenton process [20,21]. CWPO employs H_2O_2 and transition metals (mostly $Fe^{3+}_{(s)}$ and $Cu^{2+}_{(s)}$) immobilized on different solid phases [22,23], which act as catalysts in the heterogeneous Fenton process (Eqs. 1–2) to generate reactive oxygen species (ROS), mainly hydroxyl radicals (HO•). The generated ROS can attack the natural organic matter even until reach their complete mineralization (conversion to CO_2) (Eq. 3) [24].

$$Fe^{2+} + H_2O_2 \rightarrow HO^{•} + Fe^{3+} + OH^{-} \quad \text{Fenton reaction} \quad (1)$$

$$Fe^{3+} + H_2O_2 \rightarrow HO_2^{•} + Fe^{2+} + H^{+} \quad \text{Fenton} - \text{like reaction} \quad (2)$$

$$RH(\text{organic substrate}) + ROS \rightarrow \text{intermediates} \rightarrow CO_2 + H_2O + by - products \quad (3)$$

In our previous studies [25], the use of Al/Fe-pillared clays as CWPO catalysts showed to be particularly effective. In fact, owing of its low cost and high stability against the active metal leaching. CWPO displayed an excellent performance (~90 % color removal and dissolved organic carbon mineralization) even from real surface water samples [17].

The natural organic matter (NOM) is considered the foremost precursor of DBP [26]. NOM is a complex mixture of aromatic and aliphatic hydrocarbon structures bearing different functional groups [27]. NOM can be classified by its polar character in hydrophobic (HPO), hydrophilic (HPI), and transphilic (TPI) fractions [28]. According to Hua et al. [29], the hydrophobic fraction in the samples is mainly represented by humic acids or compounds containing a large number of aromatic carbons, phenolic structures, and conjugated double bonds, whereas the hydrophilic fraction contains compounds having abundant carboxylic, carbonylic, and hydroxylic functions, preferentially linked to aliphatic chains [30]. Finally, the transphilic fraction is represented by compounds of intermediate polarity between hydrophobic and hydrophilic fractions [31]. Although much research has been done on this topic, there is no general agreement about which fraction of NOM is the one most responsible for THM and HAA formation [32]. Hydrophobic [33,34] and hydrophilic [35] fractions have pointed out to be the main precursor for disinfection by-products. In another cases, such the electro-peroxone AOP, under certain conditions, the NOM residual fractions can be more reactive to form THM and HAA [36]. It is therefore important, study the advanced oxidation process, not only from the effective degradation of natural organic matter but from its effects on changes in NOM properties and the consequent impacts on DBP formation in the post-chlorination process, a topic with large current knowledge gaps, mainly in the quantification of reactive moieties of NOM. As was mentioned in a recent review study of this topic addressing UV-based advanced oxidation processes [15].

To the best of our knowledge, no study has been done on the influence of CWPO, as a pre- or post-treatment to improve NOM's removal, with subsequent DBP's prevention, in DWTPs. Accordingly, in this study, water samples were taken from two DWTPs in *Nariño*, Colombia: (1) a DWTP supplied by a raw water source with predominant hydrophobic character, and (2) a DWTP from a raw water source having a highly hydrophilic character. Then, the CWPO treatment was applied on different points of each plant: raw water source, effluent of the physicochemical treatment, and effluent of chlorination. CWPO was tested at natural pH, using Al/Fe-PILC clay as catalyst and H_2O_2 as oxidant. It was compared the extent of THM and HAA formation. Because of both their recurrence in surface water samples and their relative high toxicity [37], the total THM measured were bromodichloro-, dibromochloro-, trichloro-, and tribromomethane, while the HAA measured were monochloro-, dichloro-, trichloro-, monobromo-, dibromo-, and

tribromoacetic acids. NOM fractionation and distribution of molecular weights were carried out for both untreated and CWPO-treated water samples to trace NOM degradation, and also to examine the effect of the NOM's polar fraction and the range of molecular weights on the HAA and THM formation.

2. Experimental

2.1. Chemicals

In the fractionation of NOM by liquid column chromatography, XAD-4 and DAX-8 Amberlite type no-ionic resins (Sigma-Aldrich) and sodium hydroxide (NaOH 98 %, Panreac) were used. To study the molecular weight distributions of the dissolved organic matter, polystyrene sulfonate (Phenomenex) standards were employed and sodium chloride (NaCl 0.1 M, 99.99 %, Sigma-Aldrich) to fix the ionic force of the samples. Sodium hydrogen phosphate (Na_2HPO_4, 99.0 %, Panreac)/sodium dihydrogen phosphate (NaH_2PO_4, 99.0–100.5 %, Panreac) were used to prepare phosphate buffer (pH ~ 7.0). In the catalytic experiments, a previously characterized aluminum/iron pillared clay catalyst (Al/Fe-PILC$_{technical}$ from now Al/Fe-PILC) [17] was used. This catalyst exhibited the following main properties: d_{001} (powder XRD) 1.67 nm, BET specific surface (S_{BET}) 153 m^2/g, microporous surface ($S_{\mu p}$) 110 m^2/g, incorporated aluminum 1.42 % w/w, and incorporated iron 1.72 % w/w. Hydrogen peroxide (H_2O_2, 50 %, Sigma Aldrich) was used as an oxidant. Sodium hypochlorite (NaClO, 15 %, Bio pharChem) was employed to chlorinate the water samples and sodium thiosulfate ($Na_2S_2O_3$, 99.0–100.5 %, Panreac) was used to stop the reaction between the NOM and chlorine at the desired time [38]. The total THM studied were trichloromethane ($CHCl_3$) or chloroform, bromodichloromethane ($CHBrCl_2$), dibromochloromethane ($CHBr_2Cl$), and bromoform ($CHBr_3$). These were included in the 501 Trihalomethane Mix standard, with 200 μg/mL of each in methanol (Restek). The solvents *n*-Pentane (C_5H_{12}, ≥99.8 %, Merck) and methyl-tert-butyl-ether (MTBE) ($C_5H_{12}O$, ≥99.8 %, Merck) were used in liquid-liquid extractions of THMs and HAAs. The HAAs studied were monochloroacetic acid ($CH_2ClCOOH$), dichloroacetic acid ($CHCl_2COOH$), trichloroacetic acid (CCl_3COOH), monobromoacetic acid ($CH_2BrCOOH$), dibromoacetic acid ($CHBr_2COOH$), and tribromoacetic acid (CBr_3COOH). These were included in the 552.3 Haloacetic acid standard, with 1000 μg/L of each in MTBE (Restek), in order to standardize the derivatization conditions of the acids. The haloacetic acid methyl ester Mix #1 standard, with 1000 μg/L of each of the acids in their methyl ester forms in MTBE (Restek) were used to develop the chromatographic method. Methanol (CH_3OH, ≥ 99.8 %, Merck) and sulfuric acid (H_2SO_4, 98 %, Panreac) were used in the derivatization of the haloacetic acids. All reagents were used as received.

2.2. Sampling at DWTPs

Samples were collected, in multiple sampling trip, from the following main municipalities of *Nariño* province, southwest Colombia: *Pasto* (1°12′52″N, 77°16′41″W; altitude: 2527 m above sea level (masl); average temperature: 12 °C) and *Túquerres* (1°05′14″N, 77°37′08″W; altitude: 3104 masl; average temperature: 11 °C).

The sampling was carried out in two drinking water treatment plants that use conventional physicochemical treatment including coagulation/flocculation/sedimentation/filtration and disinfection by the addition of chlorine.

Samples from the *Pasto* and *Túquerres* treatment plants were taken at three points: in the raw water (*rw*), in the effluent of the physicochemical treatment stage (*ep*) and in the effluent of the chlorination treatment stage (*ec*), making up a total of 3 samples for each plant. In all cases, the samples were collected in amber glass containers with Teflon lined screw caps. They were kept at 4.0 °C during transportation and until analysis. Sodium thiosulfate (100 mg/L) was added to samples that

came from the chlorination treatment effluents [39].

2.3. NOM characterization of real water samples

2.3.1. Recorded physicochemical properties of NOM

The samples were characterized by absorbance at 254 nm (UV_{254}) in a Shimadzu 2600 spectrophotometer to calculate the overall NOM aromatic content [37]. The samples were previously filtered at 0.45 μm and analyzed in a Shimadzu TOC-L CPH analyzer to determine the dissolved organic carbon (DOC), by the non-purgeable organic carbon (NPOC) method in the presence of a high sensitivity platinum catalyst (detection limit: 4.0 μg C/L) ideal for measuring low concentrations of organics in water samples. Specific ultraviolet absorbance (L/mg·m) was calculated as follows: $SUVA_{254} = [UV_{254} (cm^{-1}) / DOC (mg/L)] \times 100$.

2.3.2. Fractionation and molecular weight distribution of NOM

The NOM contents were fractionated into hydrophobic (HPO), transphilic (TPI) and hydrophilic (HPI) fractions by adsorption onto DAX-8 and XAD-4 resins, in accordance with the procedure reported previously [40]. The method was set up using a synthetic surrogate of NOM containing HPO, HPI and TPI fractions (Table S1).

The resins were washed with ultrapure type I water (0.055 μS/cm of conductivity) and conditioned at pH 2.0 with H_3PO_4 0.1 M. 100 mL of water samples were acidified and filtered with qualitative paper (~8–12 μm) (BOECO-Germany FTR 3.303.185 grade 3 hw/Filter discs) to remove suspended solids. Each water sample was then passed through a DAX-8 column and the non-retained fraction was fed into a XAD-4 column. Each fraction was then retained in either DAX-8 or XAD-4 and was eluted with NaOH 0.01 M. The DOC content and the UV_{254} absorbance were recorded for each NOM fraction.

The molecular weight (MW) distributions were measured by size exclusion chromatography (HPLC-SEC) [41,42] using both a refractive index (RID) and photometric diode array (PDA) detectors (Prominence, Shimadzu); the samples were previously filtered at 0.45 μm. The injection volume was 100 μL, and a TSKGel G3000 PWXL (30 cm × 7.8 mm) column was used. The temperature of the column was 30 °C, at a flow of 0.5 mL/min, and the mobile phase was phosphate buffer (NaH_2PO_4/Na_2HPO_4) pH ≈ 7.0 with 0.1 M NaCl. A calibration curve was built using several polystyrene sulfonate standards and acetone between 0.058 and 2017 kDa (Log MW $= -0.006X^3 + 0.295X^2 - 5.276X + 35.234$; X: Retention time; $R^2 = 0.985$).

2.4. Catalytic experiments

The catalytic experiments were performed as previously reported [43] on the *rw*, *ep*, and *ec* samples from two DWTP (*Pasto* and *Túquerres*), at the pH and temperature recorded at each sampling point. 475 mL of every water sample were put into a 1.5 L glass reactor under constant mechanical stirring; hydrogen peroxide (H_2O_2) solution and the clay catalyst (Al/Fe-PILC, 60 mesh) were then added at (3.7 mg H_2O_2/mg DOC) dosage and the equivalent amount to provide 3.8 mg Fe/L. H_2O_2 was added stepwise at ~0.56 mL/min for 3 h, corresponding to the full assessed reaction time. The total time employed in each catalytic test was 4 h. The additional hour was distributed between 30 min at the beginning for pre-equilibrium between the NOM solution and the catalyst surface (without peroxide) and 30 min once finished the H_2O_2 addition to promote full reaction of the oxidizing reagent. The initial and final samples of each CWPO catalytic test were fractionated according to their polar character and stored for chlorination. Samples previously filtered at 0.45 μm were analyzed to determine UV_{254} and DOC content. HPLC-SEC analyses were then carried out.

2.5. Disinfection by-products formation

2.5.1. Chlorination of water samples

100 or 50 mL of untreated and CWPO-treated samples, as well as their corresponding fractions, were chlorinated with 10 mg/L NaClO in accordance with [15,44]. The dose employed was to ensure the free chlorine levels to be in the range 0.3–2.0 mg/L. The free chlorine was measured using a HI93701–1 reagent powder kit. In addition, 1.0 mL of phosphate buffer (pH 7.4) was added on 50 mL of the sample before chlorination. For *rw* and *ep* water samples, chlorination was carried out in the laboratory as show below:

(Without CWPO treatment): Water sample (*rw*, *ep*) → chlorination in lab → THMs and HAAs determination

(With CWPO treatment): Water sample (*rw*, *ep*) → CWPO → chlorination in the lab → THMs and HAAs determination

Chlorination of the *ec sample* was already made in the DWTP, so only the CWPO test in this case was applied.

(Without CWPO treatment): Water sample (*ec*) → THMs and HAAs determination

(With CWPO treatment): Water sample (*ec*) → CWPO → THMs and HAAs determination

After CWPO treatment, THM and HAA formation were both recorded by storing samples in the dark for 24 h before measurement.

2.5.2. THM and HAA determinations

The THMs were separated by liquid-liquid extraction using MTBE based on an adaptation of a previously reported method [45]: 10 mL of the sample were poured onto a 50 mL separating funnel, then 4 mL of MTBE were added and the mixture was stirred for 30 s. The mixture was left to rest for 2 min until the separation of two phases. The aqueous phase was removed, and the organic phase was reserved for chromatographic analysis.

Before their analyses, the HAAs were derivatized to their methyl esters [46,47]. The HAA derivatization consisted of acidifying 10 mL of sample with 2.0 mL of H_2SO_4 to maintain pH ≤ 0.5. After that, 2.0 mL of a methanol:sulfuric acid solution (9:1) were added and the solution was heated in a thermoreactor at 50 °C for 2 h. The solution was then put in an ice bath for 5 min and the content was transferred into a separation funnel. Afterwards, 4.0 mL of $NaHCO_3$ (1.06 M) and 5.0 mL of Na_2SO_4 (1.01 M) were added, followed by 4.0 mL of MTBE. The mixture was then stirred for 5 min and held steady for 1 min. The extract obtained was then analyzed. Both series of DBP were measured by gas chromatography equipped with an electron capture detector (GC/ECD) in a GC-2010 PLUS Shimadzu instrument, under the chromatographic conditions previously reported [45]. To determine the THMs, the injector temperature was fixed at 250 °C, the split ratio was set at 15.0 and the following column oven program was used: the initial temperature was 40 °C (4 min), then it was increased to 90 °C (3 °C/min), and finally it was increased at a rate 60 °C/min up to 200 °C (3 min), with a linear speed of 25.3 cm/s. The detector temperature was 270 °C. The total time per run was 22.5 min. To determine the HAAs, the injector temperature was fixed at 250 °C, the split ratio was set at 25.0 and the following column oven program was used: the initial temperature was 40 °C (1 min), then it was increased to 100 °C (4 °C/min) and maintained for 1 min, and finally it was increased at 20 °C/min up to 220 °C (2 min), with a linear speed of 25.6 cm/s. The detector temperature was 330 °C. The total time per run was 25 min. The carrier gas was N_2 (99.999 %), with a 40 mL/min constant flow for the THMs and a 30 mL/min for the HAAs. A Rxi-5Sil MS (30 m × 0.25 mm i.d × 0.25 μm film thickness) (Restek) capillary column was employed for both determinations. Calibration curves were plotted in a range of 2–200 μg/L for each analyte THM and HAA series. An MTBE blank was used for daily quality control. Linearity was considered adequate when the coefficients of determination (R^2) were ≥0.999 for THMs and ≥0.999 for HAAs. The limits of detection were established in a range of 2.32–4.05 μg/L for the THMs and 4.00–5.68 μg/L for the HAAs, while limits of quantification were

established in a range of 2.32–4.15 µg/L for the THMs and 4.93–6.58 µg/L for the HAAs, respectively.

3. Results and discussion

3.1. NOM fractions, THMs and HAAs contents through the conventional treatment stages in the DWTPs

The fractions of NOM and disinfection by-products were assessed at the three sampling points (*rw*, *ep* and *ec*) in the two DWTPs studied (*Pasto* and *Túquerres*).

3.1.1. Characteristics of the water sources

As can be seen in Table 1, the water supplies of both treatment plants displayed quite different characteristics. Raw water from the *Pasto* plant (*rw-Pasto*) showed a high aromatic content: $UV_{254} = 0.211 \pm 0.001$ cm^{-1}, DOC content $= 4.310 \pm 0.003$ mg C/L, and specific UV_{254} absorbance ($SUVA_{254}$) exceeding 4.0, indicating a predominantly hydrophobic character [29]. In contrast, the raw water from *Túquerres* (*rw-Túquerres*) exhibited a $SUVA_{254}$ lower than 2.0, characteristic of a hydrophilic character. This sample displayed $UV_{254} = 0.025 \pm 0.001$ cm^{-1} and DOC $= 1.939 \pm 0.152$ mg C/L contents lower than the raw water supplying the *Pasto* plant.

When the characteristics of the *rw* samples are compared with those of the *ep* samples, the effects of the physicochemical treatment can be observed. In this sense, the physicochemical treatment at the *Pasto* plant achieved the removal of 83 % of the aromatic content and 22 % of DOC, which implies that the treatment was efficient breaking bonds responsible of aromaticity, but not mineralizing completely the compounds. Meanwhile, for the *Túquerres* plant, the physicochemical treatment showed to be not very efficient where the DOC, UV_{254}, and $SUVA_{254}$ values remained almost constant. These results are probably related to: (1) the low turbidity (2.0 NTU) of the source water, and (2) the largely hydrophilic nature of NOM. Low turbidity implies a higher coagulant consumption and an inefficient final separation. In this type of samples, the few particles in suspension that are usually stable do not easily collide with each other, preventing the formation of an effective aggregate. Therefore, when formed, flocs are usually small and break easily [48]. In addition, hydrophilic NOM fraction affects the development of coagulation [49] since it usually exhibits a significantly lower charge density and a lower molecular weight than the hydrophobic one. Thus, the conventional physicochemical treatment of water with low turbidity and hydrophilic character, as is the case of the *Túquerres* plant, constitutes a technical challenge.

3.1.2. NOM fractions in water sources

The presence of the hydrophobic, hydrophilic and transphilic fractions of NOM was identified, with results in good agreement with the $SUVA_{254}$ values obtained for the water sources.

The distribution of NOM fractions in each sample for both plants is shown in Fig. 1. It was observed that the physicochemical treatment stage largely removed the hydrophobic fraction at the *Pasto* DWTP. For the *Túquerres* DWTP, the treatment did not achieve any considerable effect on the hydrophobic and hydrophilic fractions, due to the nature of the surface water source. There was a slight transformation between the transphilic and hydrophilic fractions after the treatment, without significant DOC removal. This transformation was also evidenced in the *Pasto* plant but to a lesser extent, which is in good agreement with the findings of Tubic et al. [32], who suggested that some of the transphilic fraction from the raw water is transformed into the hydrophilic fraction during FeCl$_3$/polyaluminum chloride coagulation. At the *Pasto* and *Túquerres* DWTPs, polyaluminum chloride and granulated aluminum sulfate are regularly used as coagulants, respectively. It is possible that such a transformation between the NOM fractions could also be observed.

Finally, the chlorination stage of treatment in both DWTPs caused the opposite transformation in comparison to the physicochemical treatment. In other words, a transformation from the hydrophilic fraction into the transphilic fraction in the final (already chlorinated) effluent (*ec-Pasto* and *ec-Túquerres*) was observed. In this sense, Sanchis et al. [50] reported that chlorination produces significant changes in NOM; high resolution mass spectrometry indicated the appearance of highly oxidized species in the tannin-like region, which could be associated with structures of transphilic character. Therefore, while it was observed that the physicochemical treatment can generate a slight conversion of the transphilic into the hydrophilic fraction, with the chlorination treatment the inverse effect from hydrophilic to transphilic character takes place.

3.1.3. THMs and HAAs in water samples

The determination of the THMs and HAAs formed in each type of water (*rw*, *ep* and *ec*) indicates the relative reactivity of NOM and its fractions at each stage of the conventional DWTP. Table 2 displays the total concentrations of THMs and HAAs (total THMs and total HAAs, respectively) found both for samples taken at the DWTPs and for those chlorinated in the laboratory. For the samples taken at the DWTPs, no THMs or HAAs were detected in the raw water (*rw*) or the effluents of the physicochemical stage of treatment (*ep*) at both plants. However, THMs and HAAs were found in the chlorinated effluents at both plants. It is worth noting that the final effluent of *ec-Pasto* exceeded the maximum allowed values of total THMs (80 µg/L) and total HAAs (60 µg/L) by the US-EPA, which suggest very interesting to test the coupling of the treatment system with the CWPO process.

When the chlorination of the samples (*rw* and *ep* taken at the plants) was carried out in the laboratory, it was observed that the specific total concentrations of THMs (Table 2) were higher for the *ep* samples than for the *rw* samples in both plants ($[THM]_{ep} > [THM]_{rw}$). In the case of the haloacetic acids, the same trend was observed in *Túquerres* plant ($[HAA]_{ep} > [HAA]_{rw}$), whereas these by-products remained constant for both types of water at *Pasto* DWTP.

Table 1

Properties of real surface water samples taken from three sampling points at the *Pasto* and *Túquerres* drinking water treatment plants.

Water source[a]	T[b] (°C)	pH	UV_{254} (cm^{-1})	DOC[c] (mg C/L)	$SUVA_{254}$[d] (L/mg DOC·m)	Main NOM fraction
rw-Pasto	14.1 ± 0.1	7.38 ± 0.11	0.211 ± 0.001	4.310 ± 0.003	4.90 ± 0.03	Hydrophobic
rw-Túquerres	15.0 ± 0.1	7.43 ± 0.03	0.025 ± 0.001	1.939 ± 0.152	1.28 ± 0.15	Hydrophilic
ep-Pasto	13.9 ± 0.1	7.49 ± 0.10	0.036 ± 0.001	3.361 ± 0.438	1.07 ± 0.16	Hydrophobic
ep-Túquerres	16.0 ± 0.1	7.06 ± 0.12	0.025 ± 0.003	2.081 ± 0.172	1.20 ± 0.20	Hydrophilic
ec-Pasto	13.3 ± 0.1	7.35 ± 0.10	0.028 ± 0.001	3.421 ± 0.483	0.82 ± 0.15	Hydrophobic
ec-Túquerres	16.0 ± 0.1	7.79 ± 0.06	0.046 ± 0.009	1.990 ± 0.043	2.31 ± 0.50	Transphilic

[a] Sampling points at the plants: raw water (*rw*), in the effluent of physicochemical coagulation/flocculation treatment stage (*ep*), in the effluent of chlorination treatment stage (*ec*).

[b] T: temperature at sampling location.

[c] DOC: dissolved organic carbon.

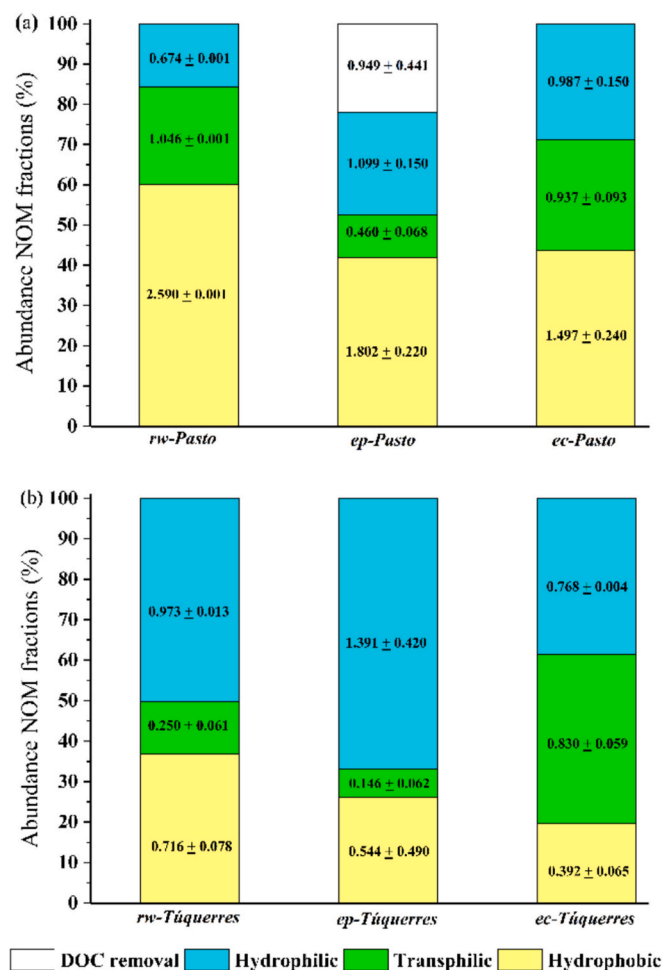[d] $SUVA_{254}$: specific UV_{254} absorbance

Fig. 1. NOM fractions at the drinking water treatment plants: (a) *Pasto* DWTP, and (b) *Túquerres* DWTP (DOC content in each fraction is also shown).

Although several reports state that NOM removal in general leads to decrease formation of disinfection by-products, the results in this study suggest a significantly different reactivity of the residual NOM fractions towards formation of THMs and HAAs. To address this properly, total THMs and total HAAs were analyzed as a function of the NOM fractions present.

3.1.4. Reactivity of the NOM fraction towards THMs and HAAs formation

As above mentioned (Section 3.1.1), the conventional treatment in the *Pasto* DWTP removes DOC. It is mainly represented by the hydrophobic fraction with average molecular weights ~6.2 kDa and ~661 kDa (Fig. S1a, supplementary material). Although the residual HPO

fraction could clearly be responsible for the formation of THMs, given the high elimination of this fraction during the physicochemical treatment, the increases in THMs in *ep-Pasto* with respect to *rw-Pasto* could be mainly attributed to the contribution of the hydrophilic fraction which increased after the physicochemical treatment (Fig. 1a). This is mostly represented by the formation of low molecular weight compounds.

For *ep-Túquerres*, the increase in THMs with respect to *rw-Túquerres* was attributed to the same observed in *Pasto* DWTP. The hydrophilic fraction increased from 0.973 mg C/L to 1.391 mg C/L (Fig. 1b). As a result, the hydrophilic and transphilic fractions in *ep-Túquerres* represented 74 % of the NOM present in the sample and at the same time there was an almost threefold increase in the concentration of THMs,

Table 2
Total THMs and total HAAs in raw water (*rw*), in the effluent of the physicochemical treatment stage (*ep*) and in the effluent of the chlorination treatment stage (*ec*) at the *Pasto* and *Túquerres* drinking water treatment plants.

Water source	Samples taken at the plants		Chlorination of the samples in the laboratory		Specific total concentrations of THMs and HAAs	
	Total THMs (µg/L)	Total HAAs (µg/L)	Total THMs after Cl$_2$ (µg/L)	Total HAAs after Cl$_2$ (µg/L)	Total THMs (µg/mg DOC)	Total HAAs (µg/mg DOC)
rw-Pasto	ND	ND	185.9 ± 0.09	291.6 ± 0.28	43.13 ± 0.05	67.66 ± 0.11
rw-Túquerres	ND	ND	25.93 ± 0.14	46.20 ± 0.07	13.37 ± 1.12	23.83 ± 1.90
ep-Pasto	ND	ND	234.0 ± 0.16	219.7 ± 0.09	69.62 ± 9.12	65.37 ± 8.52
ep-Túquerres	ND	ND	80.13 ± 0.11	69.52 ± 0.09	38.51 ± 3.23	33.41 ± 2.80
ec-Pasto	84.85 ± 0.08*	148.2 ± 0.09*	–	–	24.81 ± 3.53*	43.32 ± 6.14*
ec-Túquerres	68.13 ± 0.10*	36.33 ± 0.12*	–	–	34.23 ± 0.79*	18.26 ± 0.45*

ND: not detected.

* Chlorination in the plant.

changing from 13.37 ± 1.12 µg/L to 38.51 ± 3.23 µg/L (Table 2) for the physicochemical effluent.

As in the case of THMs, at the *Túquerres* DWTP, the specific total HAAs increased at *ep-Túquerres* (33.41 ± 2.80 µg/mg DOC) with respect to *rw-Túquerres* (23.83 ± 2.80 µg/mg DOC). This means that the transphilic and hydrophilic fractions are also reactive enough to promote HAAs formation. In *ep-Túquerres* it was found that the transphilic fraction favored the specific formation of HAAs by around 1.5 times (TPI: 456.97 µg/mg DOC, Table S2) more than the specific formation of THMs after chlorination of this fraction (TPI: 298.26 µg/mg DOC, Table S2). Moreover, the specific total HAAs for *ep-Pasto* (65.37 ± 8.52 µg/mg DOC) remained almost unchanged compared to the values found in *rw-Pasto* (67.66 ± 0.11 µg/mg DOC). In *ep–Pasto* the hydrophobic fraction was quite less reactive to HAA formation (HPO: 10.81 µg/mg DOC, Table S2) than the transphilic fraction (TPI: 101.32 µg/mg DOC, Table S2). In addition, although the hydrophilic fraction increased from *rw* to *ep* water samples (Fig. 1a), this change did not lead to increase HAA and this fraction showed to be less reactive to HAA formation.

Therefore, during the conventional treatment, the hydrophobic and hydrophilic fractions (for hydrophobic water supply), and hydrophilic and transphilic fractions (for hydrophilic water supply), showed to contribute forming THMs. In the case of HAAs, the transphilic fraction seems to be the most important contributor. In this regard, Hong et al. [51] recently suggested that water samples with extremely low SUVA$_{254}$ values may display different mechanisms forming THMs, di-HAAs and tri-HAAs compared with those with high SUVA$_{254}$ values.

The results here reported indicate that the efficient removal of the hydrophobic NOM fraction by conventional treatment leads to a decrease the content of THMs formed after disinfection, mainly due to the high reductions in DOC and the aromatic content (UV$_{254}$ and SUVA$_{254}$). In opposite behavior, the hydrophilic and transphilic fractions proved to be both resistant to conventional treatments and very reactive with chlorine, favoring the formation of THMs and HAAs. Huang et al. [52] reported that conventional treatments are not effective in the removal of hydrophilic precursors of natural organic matter and these could directly contribute to form of HAAs, where di- and tri-haloacetic acids are the HAA species with the highest concentrations in water. Therefore, both fractions (HPI and TPI) represent an important contribution to the effluent of the physicochemical treatment in DWTPs, whose removal prior to chlorination should be then a clear priority to reduce formation of the two families of harmful DBPs. It becomes even more concerning when the water source is mostly hydrophilic, since the conventional physicochemical treatments of course are not efficient enough to eliminate it completely.

3.2. Performance of the CWPO process preventing THMs formation

CWPO was applied on each of the DWTPs' treatment stages. The results summarized in Table 3 show that for the raw water (*rw*) from the *Pasto* DWTP, CWPO decreased the DOC content by 75 %, the UV$_{254}$ absorbance 80 %, and the SUVA$_{254}$ value by 36 %. Similar efficiency was recorded when the oxidizing process was applied on the *ep* sample (DOC, UV$_{254}$, and SUVA$_{254}$ values reduced by 60 %, 78 % and 22 %, respectively). This was clearly illustrated by the higher reduction in the NOM fractions for *rw-CWPO-Pasto* and *ep-CWPO-Pasto* (Fig. 2a), where the hydrophobic, hydrophilic and transphilic compounds contributing the aromatic content and SUVA$_{254}$ values were efficiently removed by the CWPO stage of treatment. Moreover, the recorded DOC removals (60–75 %) were in average higher than those reported by the coagulation/flocculation physicochemical treatment in the DWTPs (51–60 %) [32,53]. The lower decrease in the SUVA$_{254}$ value with respect to the DOC and the UV$_{254}$ contents can be explained because a fraction of HPO was effectively mineralized (converted to CO_2). Meanwhile, it seems the remaining HPO fraction was split into small fractions with aromatic moieties remaining in the sample (i.e. phenol or resorcinol type).

Furthermore, the CWPO treatment on the mostly hydrophilic *rw*

sample from the *Túquerres* DWTP also attained higher efficiency than the conventional physicochemical treatment. In the raw water, CWPO decreased the DOC content and the UV$_{254}$ absorbance by 25 % and 24 %, respectively. Meanwhile, in the physicochemical effluent (*ep*), the oxidizing treatment achieved a reduction in DOC, UV$_{254}$ and SUVA$_{254}$ of 31 %, 44 %, and 30 %, respectively.

The SUVA$_{254}$ reduction by the CWPO treatment was similar for both the mostly hydrophobic and the mostly hydrophilic water sources. However, for the hydrophobic water source, the DOC reduction was more significant than for hydrophilic water source. Therefore, in a mainly hydrophobic water source, the CWPO treatment seems to focus on the DOC removal, while in a mainly hydrophilic water, CWPO more rather achieves aromaticity removal. The efficiency shown by CWPO in both fractions can be explained by the degradation mechanism proposed in our previous study [17]. According to the proposed mechanism, the degradation in this heterogeneous catalytic system is not governed by the previous adsorption of the complex organic substrates. This, allows the hydrophobic and hydrophilic fractions, either adsorbed or not in advance, to get successfully attacked by the generated oxidizing species. It can be considered that once iron gets reduced on the catalyst's surface, the classical Fenton process becomes accelerated from the typical reaction of Fe^{2+} with H_2O_2 (Eqs. 1–3). The overall effect then increased the H_2O_2 conversion rate promoting an enhanced heterogeneous Fenton process. The generated reactive oxygen species then quickly attacked the NOM and converted it into light intermediates and by products displaying carboxylic acids and other partially oxidized organic functionalities [24].

In both DWTPs, the decrease in all parameters was more significant for the treatment on the *rw* and *ep* samples than for the chlorination effluents (*ec*). It is worth mentioning that coupling of the CWPO at the end (after chlorination) was disregarded in previous studies [17] primarily based in the DOC mineralization, taking into account that the chloride anions formed during the disinfection process are well-known scavenging species of the highly oxidizing species such as the hydroxyl radicals [54]. Moreover, in this study a smaller decrease in THM concentration was observed for the *ec* samples than for *rw* and *ep*. Therefore, henceforth the discussion will focus on how CWPO is applied on the *rw* and *ep* stages of conventional treatment to prevent the formation of both recorded families of DBPs rather than to degrade the DPBs already formed in the physicochemical stage of the DWTPs.

It accordingly suggests that the removal of the hydrophilic/transphilic NOM fractions is a crucial factor to choose the most appropriate stage of treatment at DWTPs where a CWPO unit can be coupled. Therefore, the THMs and HAAs formed were correlated with the NOM fractionation after the CWPO treatment.

### 3.2.1. Formation of THMs after CWPO treatment

THM formation was determined by measuring total and single THMs in the samples (*rw*, *ep*, and *ec*) at both plants before and after CWPO, as shown in Fig. 3. The results demonstrated that the CWPO treatment achieved a significant reduction in total THMs formation (21 %–77 %) in the hydrophobic water of the *Pasto* DWTP (Fig. 3a), and (43 %–81 %) in the hydrophilic water of the *Túquerres* DWTP (Fig. 3b), depending on the stage of treatment at which the oxidizing process was coupled; the reduction was higher than that achieved by any of the conventional steps of coagulation/flocculation conventional treatment, irrespective the polar nature of the water source. Alongside, it is worth noting that in all CWPO treated samples, the total formed THMs were below the international regulations, which can be attributed to the DOC removal (represented by the hydrophobic, hydrophilic, and transphilic fractions).

The THMs found (before and after CWPO) at the three sampling points and the two DWTPs were trichloromethane and bromodichloromethane. The formation of trichloromethane is favored by the presence of hydrophobic fractions with aromatic, methyl and guaiacyl lignin groups [55]. On the other hand, it has been reported that hydrophilic

Table 3

Properties of real surface water samples from the *Pasto* and *Túquerres* drinking water treatment plants after the CWPO treatment.

Water source[a]	T[b] (°C)	pH	UV$_{254}$ (cm^{-1})	DOC[c] (mg C/L)	SUVA$_{254}$[d] (L/mg DOC·m)	Total THMs (µg THMs/mg DOC)	Total HAAs (µg HAAs/mg DOC)
rw-CWPO-Pasto	14.1 ± 0.1	6.82 ± 0.67	0.042 ± 0.011	1.090 ± 0.01	3.12 ± 0.85	44.50 ± 1.22	49.74 ± 0.55
rw-CWPO-Túquerres	15.0 ± 0.1	6.72 ± 0.03	0.019 ± 0.001	1.450 ± 0.01	1.31 ± 0.08	3.323 ± 2.14	10.97 ± 0.20
ep-CWPO-Pasto	13.9 ± 0.1	6.94 ± 0.03	0.008 ± 0.005	1.330 ± 0.02	0.83 ± 0.53	40.50 ± 1.69	ND
ep-CWPO-Túquerres	16.0 ± 0.1	6.52 ± 0.04	0.014 ± 0.002	1.430 ± 0.02	0.84 ± 0.13	32.15 ± 1.79	56.35 ± 0.84
ec-CWPO-Pasto	13.3 ± 0.1	6.66 ± 0.02	0.015 ± 0.001	1.810 ± 0.01	0.83 ± 0.06	37.02 ± 0.63	38.92 ± 0.32
ec–CWPO–Túquerres	16.0 ± 0.1	7.10 ± 0.10	0.029 ± 0.003	1.730 ± 0.03	1.85 ± 0.22	20.87 ± 1.87	ND

Not detected (ND).

[a] Raw water (*rw*), effluent of physicochemical treatment stage (*ep*), effluent of chlorination treatment stage (*ec*), CWPO: catalytic wet peroxide oxidation.

[b] T: temperature at sampling location.

[c] DOC: dissolved organic carbon.

[d] SUVA$_{254}$: specific UV$_{254}$ absorbance
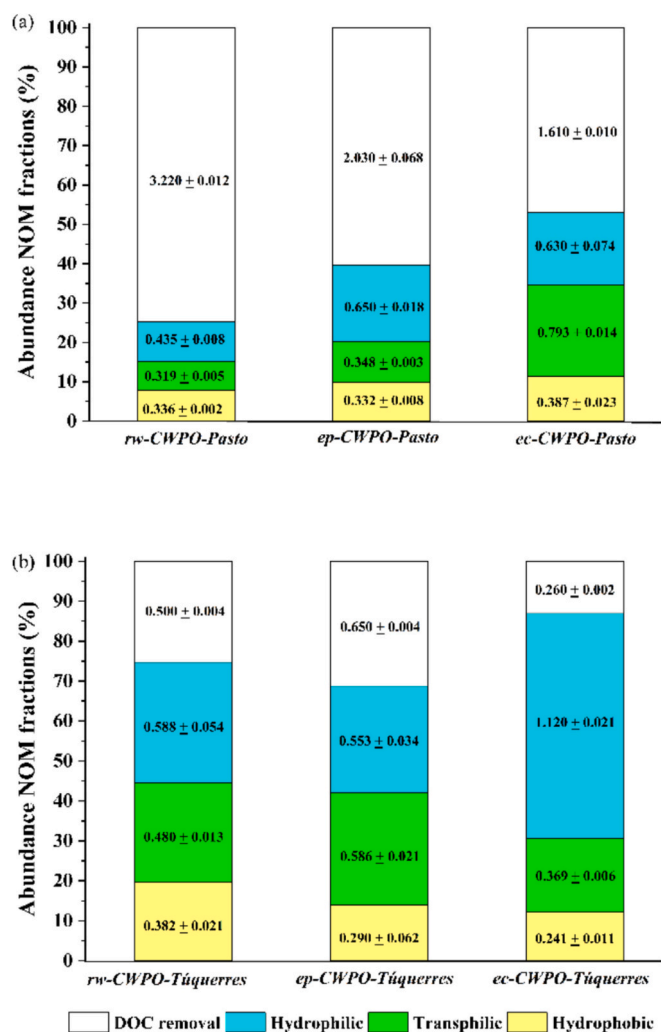
Fig. 2. NOM fractions and DOC removal at drinking water treatment plants after the CWPO treatment: (a) *Pasto* DWTP, and (b) *Túquerres* DWTP. DOC content in each fraction is also shown.

fractions of NOM are more likely incorporating bromine [56], which explains the additional presence of dibromochloromethane in *ep-Túquerres* (Fig. 3b). Therefore, because of the more hydrophilic character of the water supply of the *Túquerres* plant, the formation of brominated-THMs was favored there. However, this compound was not found in the effluent treated by the CWPO process.

The significant reductions in THM formation after CWPO for *rw* and *ep* of *Pasto* DWTP (Fig. 3a) were very similar, 74 and 77 %, respectively (for *rw-Pasto* there was a decrease from 185.9 µg/L to 48.51 µg/L, whereas for *ep-Pasto* from 234.0 µg/L to 53.87 µg/L). In the case of the *Túquerres* DWTP, the lowest total concentrations of the THMs (Fig. 3b) were observed after applying CWPO on the *rw* sample (from 25.93 µg/L to 4.819 µg/L) with an 81 % of THMs mitigation.

3.2.2. Correlation of NOM fractions with the formation of THMs

The CWPO was very efficient in the removal of NOM fractions in both DWTPs. The NOM fractions present in each water sample after the CWPO treatment are shown in Fig. 2.

In the case of *rw-CWPO-Pasto*, the CWPO treatment removed more HPO (87 %) and TPI (70 %) than HPI fraction (36 %) (Fig. 3a). These are significantly higher removal rates than those reported to take place in other efficiently coupled AOPs; for instance, an iron–carbon micro electrolysis column/up-flow biological aerated filter achieved 53 % and 56 % removal for the HPO and TPI fractions, respectively [57]. In the case of *rw-CWPO-Túquerres,* there were similar removals of the HPO (47 %) and HPI (40 %) fractions (Fig. 3b) after the oxidizing treatment and a slightly higher removal of the HPI fraction than in the *Pasto* plant, probably due to the presence of a larger amount of this fraction in the water source. It can be related with the significant reduction in the formation of THMs of 81 % for *rw-CWPO-Túquerres* compared to 74 % for *rw-CWPO-Pasto* (Fig. 3). High percentages of THMs mitigation were achieved irrespective the nature of the source and the concentration of THMs formed without the oxidizing treatment, considering that the THMs concentration in the source water supplying *Pasto* was almost 10 times higher than in source water of *Túquerres*.

The CWPO on *ep-Pasto* (*ep-CWPO-Pasto*) achieved the removal of a slightly higher percentage of the HPI fraction (41 %) than the CWPO on *rw-Pasto* (36 %). Furthermore, most of the HPO fraction (82 %), and 24 % of the TPI fractions were removed in *ep-CWPO-Pasto* (Fig. 2a). However, the formation of THMs (Table 3) was very similar in *ep-CWPO-Pasto* (THMs: 40.50 ± 1.69 µg/mg DOC) and *rw-CWPO-Pasto* (THMs: 44.50 ± 1.22 µg/mg DOC). This is because the final distribution of the three fractions after applying CWPO on either *rw* or *ep* was very similar (Fig. 2a), and the order reactivity of the overall fractions did not significantly change after the CWPO treatment (Table S2).

In the case of *ep-CWPO-Túquerres*, CWPO removed more hydrophilic (60 %) than hydrophobic (47 %) fractions. In addition, an increase in the TPI fraction was observed after treatment. As already mentioned, here it is worth noting the more hydrophilic nature of the water supply of the *Túquerres* DWTP. Thus, in water samples with low SUVA$_{254}$ values, the CWPO treatment may play an important role in the transformation of functional groups of either hydrophobic or hydrophilic moieties into transphilic groups. A similar behavior was observed in the transformation of hydrophobic groups into hydrophilic ones, like in the case of ozonation [57]. In this case, a transformation from a mainly hydrophilic into a transphilic fraction took place, where after CWPO the TPI fraction in *ep-CWPO-Túquerres* was greater than in *ep-Túquerres*, perhaps as a consequence of a higher HPI fraction in the input stream of *ep-*
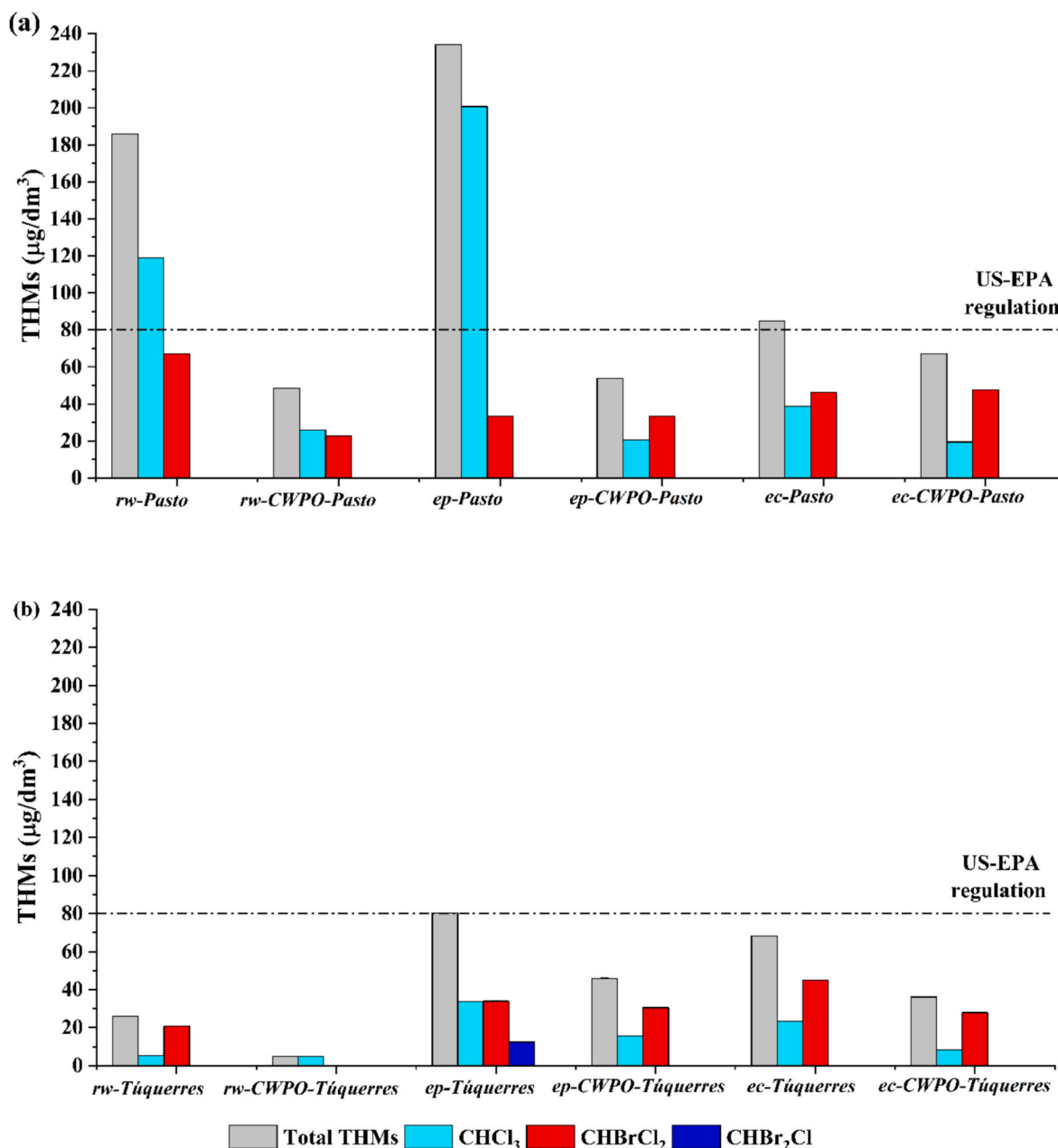
Fig. 3. Formation of total and single THMs after chlorination of the samples from (a) *Pasto*, and (b) *Túquerres* DWTPs with and without previous CWPO treatment.

Túquerres (HPI: 68 %) in comparison to *rw-Túquerres* (HPI: 50 %). This seems to be closely related with the increase in total THMs in *ep-CWPO-Túquerres* (32.15 ± 1.79 µg/mg DOC) in comparison to *rw-CWPO-Túquerres* (3.323 ± 2.14 µg/mg DOC).

Either case, CWPO played a key role in breaking large-molecular-weight compounds into low-molecular-weight ones, due to the high oxidizing power of the reactive oxygen species generated by the heterogeneous Fenton process. The apparent molecular weight distribution of NOM in the CWPO-treated samples is shown in the Fig. 4. As it can be seen, the CWPO treatment on the *rw* sample of the *Pasto* DWTP mainly degraded high (~661 kDa) and low (~6.2 kDa) molecular weight organic fractions (Fig. 4a). Meanwhile, the treatment of *rw-Túquerres* also removed high molecular weight (~1000 kDa) fractions and led to lower molecular weights (<3 kDa) (Fig. 4c). A similar plot was obtained for treatment of the corresponding effluents of the physicochemical unit (*ep*), but of course, in *Pasto* plant, the heavier fractions were significantly depleted in advance by the physicochemical treatment (Fig. 4b). In this

case the oxidative treatment CWPO was efficient to degrade remaining NOM fractions (6.2 kDa). However, the physicochemical unit at the *Túquerres* plant (mostly hydrophilic character source) was less effective at depleting higher molecular weight fractions, whereas the oxidative treatment was very effective in degrading these fractions (Fig. 4d). In fact, the CWPO treatment for the *ep* from *Túquerres* almost fully removed a heavier average molecular weight at around 1000 kDa, and just partially depleted it at 6.3 kDa, leading to couple of new signals in the range of 2–3 kDa and a higher peak at 0.39 kDa.

Remarkably, the slight increase in the signal centered at 0.36 kDa MW for *ep-CWPO-Pasto* did not lead to a higher formation of THMs with respect to *ep-Pasto* (Fig. 4b), suggesting a low reactivity of this fraction as a precursor of THMs. This was confirmed by the total concentration of THMs in *rw-CWPO-Túquerres*, where the signal at 0.36 kDa intensified significantly compared with that of *rw-Túquerres* (Fig. 4c). Thus, it appears the NOM residues at around 2–3 kDa formed after the CWPO treatment of the *ep-Túquerres* sample were those mainly responsible for

its quite negligible decrease in specific total THM concentration (*ep-Túquerres*: 38.51 μg THM/mg DOC vs. *ep-CWPO-Túquerres*: 32.15 μg THM/mg DOC). It outstands in comparison with the decrease achieved for the corresponding *rw* samples from the same plant (*rw-Túquerres*: 13.37 μg THM/mg DOC vs. *rw-CWPO-Túquerres*: 3.323 μg THM/mg DOC) where the mentioned fractions were degraded after CWPO treatment. Accordingly, the formation of THMs seems to be mainly governed by two factors: *(i)* the hydrophobic character of the dissolved NOM, and *(ii)* the presence of low to intermediate molecular weight compounds (just exceeding 2 kDa). When the water source is mainly hydrophobic (like in the case of *rw-Pasto*), this fraction is the key responsible for THM formation, whereas in the presence of primarily hydrophilic NOM (for instance *rw-Túquerres*), the low to intermediate molecular weight compounds (~2.3–6.8 kDa) seem the main precursors promoting THM formation.

Finally, the CWPO treatment for both (*rw* and *ep*) effluents achieved similar final levels of THMs (*rw-CPWO-Pasto* and *ep-CWPO-Pasto*: ~0–30 μg/dm³, Fig. 3). Therefore, when the water supplies are predominantly hydrophobic, it does not significantly change the specific total concentration of THMs in the treated effluent by either treating the raw water or the physicochemical effluent with the advanced oxidation process. Meanwhile, oxidizing transformations of mainly hydrophilic NOM contents (like in the case of the *Túquerres* water supply) into low to intermediate molecular weight transphilic compounds strongly promote the later formation of THMs. Consequently, in the scenario of coupling CWPO to complement conventional DWTPs, the best stage to apply CWPO seems to be on the raw water source irrespective the polar nature of its NOM content. This idea will must be then contrasted with the

formation of HAAs after CWPO treatment at different stages of the two DWTPs.

3.3. Performance of the CWPO process preventing HAAs formation

3.3.1. Formation of HAAs after CWPO treatment

In all cases, except for sample *ep-CWPO-Túquerres*, the total concentration of HAAs (Total HAAs) successfully decreased after the CWPO treatment (Fig. 5). Depletions of 83 % and 65 % in HAAs formation were achieved when the treatment was applied over the raw waters at either *Pasto* or *Túquerres* DWTPs, respectively. However, it is remarkable that when the oxidizing treatment was applied over *ep*, 100 % depletion was obtained in the case of *Pasto* plant, whereas in *ep-CWPO-Túquerres* sample, HAAs increased around 15 %. Therefore, the contribution of the NOM fractions to the HAA formation was analyzed.

3.3.2. Correlation of NOM fractions with the formation of HAAs

As mentioned (Section 3.2.2), at *Pasto* DWTP, CWPO significantly decreased the HPO fraction in the raw water sample (Fig. 2), and despite this, in *rw-CWPO-Pasto* the highest molecular weights of NOM (primarily corresponding to the HPO fraction) got fully depleted. Although the concentration of HAAs decreased, did so in a smaller proportion than expected. The slightly decreased concentration of HAAs (from 67.66 μg HAA/mg DOC to 49.74 μg HAA/mg DOC) as a consequence of the oxidizing treatment, should be then mainly attributed to the HPI fraction exhibiting around 4.6 kDa, since HPI was present in a larger amount than any other fraction in *rw–CWPO–Pasto* (Fig. 2a), and its reactivity when forming HAAs (149.40 μg/mg DOC, Table S3) was higher than
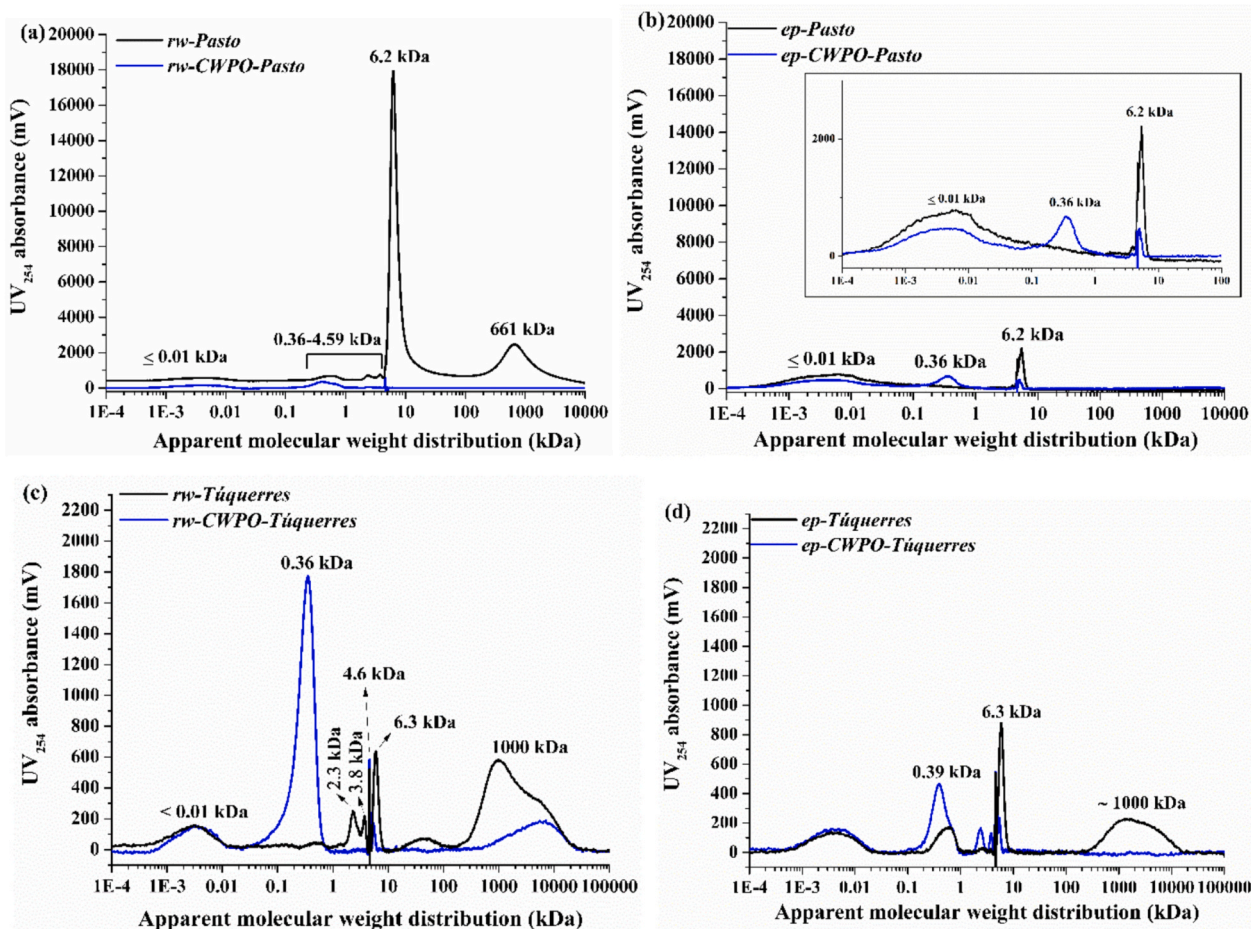

Fig. 4. Apparent molecular weight distribution of NOM before and after the CWPO treatment at points raw water (*rw*) and effluent of physicochemical treatment (*ep*) of the drinking water treatment plants: (a, b) *Pasto* DWTP, and (c, d) *Túquerres* DWTP.

those displayed by either the hydrophobic or the transphilic fractions. This agrees with previous reports [58] where it was found that tannic acid was the only compound significantly showing higher formation potential of haloacetic acids (155 µg/mg DOC) than resorcinol (a hydrophobic model molecule). In the case of the *ep* water samples, CWPO reduced the formation of HAAs more than in the *rw* samples, probably due to the significant removal of the HPI fraction.

The depletion of total HAAs in *rw-CWPO-Túquerres* in comparison to *rw-Túquerres* can be mainly ascribed to the reduction in both the HPO

and HPI fractions, alongside the removal of NOM fractions centered at 6.3 kDa and 1000 kDa (Fig. 4). Thus, the total HAAs after the CWPO treatment were primarily formed because of the TPI fraction that increased after treatment. However, the increase was more significant for *ep-CWPO-Túquerres* than in *rw-CWPO-Túquerres,* which is apparently related to the formation of low molecular weight NOM moieties represented in 2.3 kDa and 3.8 kDa, as explained previously for THMs (Fig. 4c). Furthermore, the CWPO stage for *rw-Túquerres* significantly enhanced the signal around 0.36 kDa (Fig. 4c). Nevertheless, this
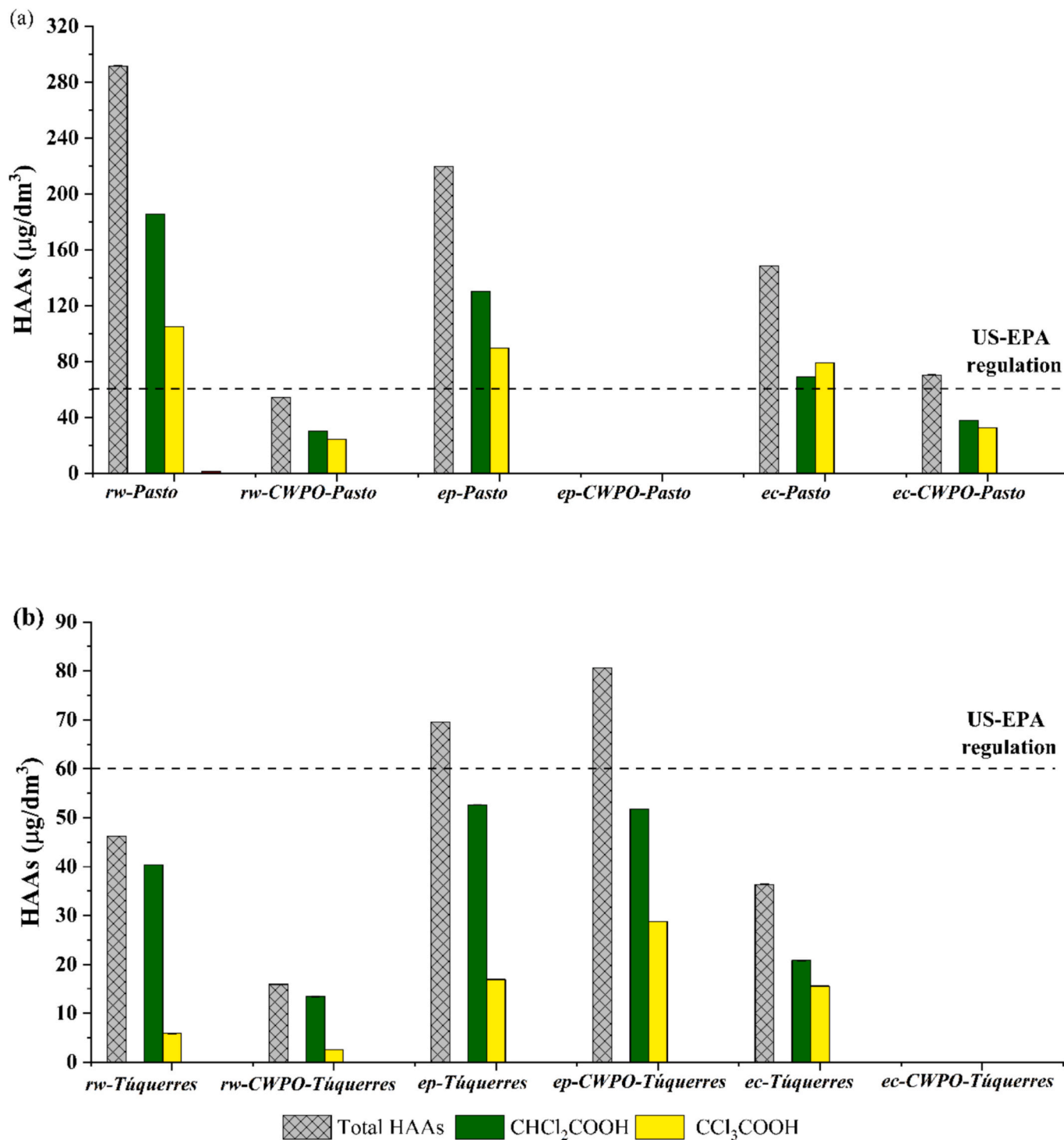

Fig. 5. Total and single concentration of HAAs after chlorination of the samples from (a) *Pasto*, and (b) *Túquerres* DWTPs with and without previous CWPO treatment.

increment did not increase the total HAA concentration, in this stage HAAs decreased from 23.83 μg HAAs/mg DOC in *rw-Túquerres* to 10.97 μg HAAs/mg DOC in *rw-CWPO-Túquerres*. The total HAAs were then more significantly reduced by the CWPO treatment over the *rw* than for the *ep* sample. Therefore, the formation of the TPI fractions of low to intermediate molecular weights in *ep-CWPO-Túquerres* showed to be the main factor increasing the total HAAs later. In this sense, Bond et al. [58] indicated that water samples with high amino acid concentrations, a common TPI fraction, are likely to raise HAA levels following AOP treatments. In such cases, a careful selection process is required for HAA control.

In this study, all NOM fractions contributed to form HAAs. However, the contribution was different depending on the type of the raw water source (very HPO vs. very HPI). Thus, the HAAs in the very hydrophobic raw water samples are mainly due to the HPO and HPI fractions. Meanwhile, in very hydrophilic raw water samples mainly are due to the HPO and TPI fractions.

3.4. Practical implications

Regarding the formation of THMs and HAAs, the present study underlines the most suitable stage of treatment at conventional DWTPs in which the CWPO application would be more advantageous (Fig. 6). It strongly depends on the $SUVA_{254}$ value of the water supply. In the case of raw waters exhibiting high values (let's say >4.0 L/mg DOC·m), it is better to apply CWPO on the effluent of the physicochemical stage, where the HPI fraction can be significantly more depleted, as well as considering the higher performance of the conventional physicochemical units of treatment at DWTPs in the removal of predominantly hydrophobic NOM loadings. As the HPO fraction gets strongly reduced, the formation of THMs upon chlorination becomes also seriously inhibited. Depletions of HPI and TPI fractions also conducted to reduce total HAAs. On the other hand, in the case of water supplies exhibiting low $SUVA_{254}$ values (let's say <2.0 L/mg DOC·m), the most suitable point of treatment could be directly on the *rw* untreated influent stream, since the increase in the transphilic fraction is lower, and fewer low to intermediate molecular weight moieties of NOM are formed after the CWPO treatment in comparison to *ep*.

These findings are also consistent with the results published in a previous study [17], where the efficiency of the CWPO treatment to complement drinking water facilities was addressed taking into account the following also important aspects: *(i)* DOC mineralization, an essential response to be maximized in order to enhance conventional DWTPs; *(ii)* the more cost-effective consumption of H_2O_2; and *(iii)* the input concentration of anions (strong scavenging substances of reactive oxygen species in the core of this family of oxidizing processes).

It is worth mentioning, the operational cost of the CWPO treatment activated by Al/Fe-PILCs in principle can be mainly ascribed to the H_2O_2 addition, since the preparation of the catalyst is relatively cheap as the starting material is a low-cost natural clay, and the material can be reused through many reaction batches. As a conclusive excerpt, the CWPO under optimal conditions of operation could be a cost-effective and feasible technological alternative improving conventional drinking water treatment plants, strongly preventing formation of hazardous disinfection by-products like the THMs and the HAAs.

4. Conclusions

In this work, the potential of the catalytic wet peroxide oxidation activated by an Al/Fe-PILC clay catalyst, to prevent formation of both THMs and HAAs after chlorination in drinking water treatment plants was established. The DWTPs studied had different polar nature of the dissolved NOM in the water supplies (very hydrophobic vs. very hydrophilic). In both cases, the CWPO treatment significantly decreased all the hydrophobic, hydrophilic and the transphilic fractions, by efficiently reducing at the same time the DOC, UV_{254}, and the $SUVA_{254}$ contents. Furthermore, the recorded DOC removal in both plants (31–75 %) were in average higher than those achieved by the coagulation/flocculation physicochemical treatment in the full-scale conventional DWTPs. Both, hydrophobic and hydrophilic fractions of NOM showed to significantly contribute forming THMs, whereas the hydrophilic, and even more strongly the transphilic fraction, were found to favor HAA's formation. The hydrophobic fraction of the dissolved NOM was preferentially mineralized into CO_2, but also partially transformed either from hydrophobic to hydrophilic/transphilic (HPI/TPI) or from hydrophilic to transphilic ones. Furthermore, the oxidative treatment played a key role in breaking large-molecular weight into low-molecular-weight compounds. It was directly reflected in the THMs and HAAs reduction after chlorination. When the oxidative treatment was previously applied over the raw water, the DWTP with the hydrophobic source displayed 74 % and 83 % less THMs and HAAs formed, respectively. In this case, the CWPO treatment mainly attained DOC removal, alongside degradation of high (~661 kDa) and low (~6.2 kDa) molecular weight organic fractions. The DWTP with the hydrophilic source displayed 81 % and 65 % for THMs and HAAs reduction, respectively. The CWPO showed to more selectively remove aromaticity and high molecular weight (~1000 kDa) fractions, leading to lighter moieties (molecular weights <3 kDa). However, CWPO applied over the effluent of the physicochemical treatment (hydrophilic source) led to a couple of new signals in the range of 2–3 kDa main responsible of HAA formation, associated at the same time with the increase of their transphilic character. This was the opposite with the hydrophobic source; in this case, CWPO over the effluent of the physicochemical treatment was also efficient to degrade the remaining NOM fractions (6.2 kDa).

Thus, catalytic wet peroxide oxidation proved to allow the degradation of natural organic matter with different polar nature at room temperature and natural pH. The proper coupling of this heterogeneous Fenton treatment, to prevent DBPs formation, can be then more easily devised as a function of the predominant polar nature of the dissolved natural organic matter fraction in the drinking water supply: *(i)* CWPO treatment on the raw water (for water supplies mainly hydrophilic, input $SUVA_{254}$ < 2.0 L/mg DOC·m), and *(ii)* CWPO treatment on the
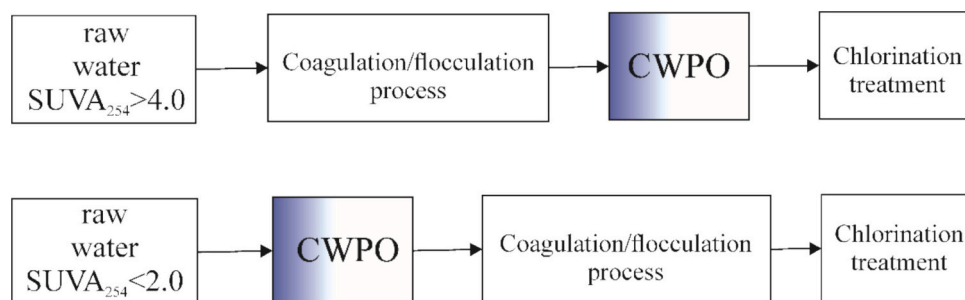

Fig. 6. Most suitable points to apply the CWPO treatment to enhance conventional drinking water treatment plants, based on the $SUVA_{254}$ displayed by the input water source.

effluent of the conventional physicochemical units at DWTPs (for water supplies mainly hydrophobic, input $SUVA_{254} > 4.0$ L/mg DOC·m).

CRediT authorship contribution statement

Omar J. Cotazo-Mosquera: Writing – original draft, Methodology, Investigation. **Viviana A. Gómez-Obando:** Methodology, Investigation. **Luis-Alejandro Galeano:** Writing – review & editing, Supervision, Resources, Methodology, Funding acquisition, Conceptualization. **Ricardo A. Torres-Palma:** Writing – review & editing, Supervision, Formal analysis, Conceptualization. **Ana M. García-Mora:** Writing – review & editing, Supervision, Methodology, Formal analysis, Conceptualization.

Funding

Declaration of competing interest

The authors declare that they have no known competing financial interests or personal relationships that could have appeared to influence the work reported in this paper.

Acknowledgments

Appendix A. Supplementary data

Supplementary data to this article can be found online at https://doi.org/10.1016/j.jwpe.2025.107335.

Data availability

Data will be made available on request.

References

[1] T. Malkoske, P. Bérubé, R. Andrews, Leveraging coagulation mechanisms to reduce fouling and increase natural organic matter removal during coagulation/flocculation-ultrafiltration treatment, Sep. Purif. Technol. 327 (2023) 124877, https://doi.org/10.1016/j.seppur.2023.124877.

[2] J. Lin, A. Ika, Minimization of halogenated DBP precursors by enhanced PACl coagulation: the impact of organic molecule fraction changes on DBP precursors destabilization with Al hydrates, Sci. Total Environ. 703 (2020) 134936, https://doi.org/10.1016/j.scitotenv.2019.134936.

[3] U.S. EPA, (US Environmental Protection Agency) National Primary Drinking Water Regulations, 2009. EPA 816-F[09]-004.

[4] IRIS, Integrated Risk Information System, Online database, U.S. Environmental Protection Agency, Washington D.C., 2008, https://iris.epa.gov/.

[5] U.S. EPA, (US Environmental Protection Agency) National Primary Drinking Water Regulations: Stage 2 Disinfectants and Disinfection Byproducts Rule Vol. 71, 2015. No 2., Washington, D.C.

[6] Health Canada, Guidelines for Canadian Drinking Water Quality: Guideline Technical Document: Trihalomethanes, 2006. Ottawa, Ontario.

[7] Health Canada, Guidelines for Canadian Drinking Water Quality: Guideline Technical Document: Haloacetic Acids, 2008. Ottawa, Ontario.

[8] European Union, Council Directive 98/83/EC of 3 November 1998 on the quality of water intended for human consumption, Off. J. Eur. Commun. 330 (1998) 32–54.

[9] Resolución 2115, Características, instrumentos básicos y frecuencias del sistema de control y vigilancia para la calidad del agua para consumo humano, Ministerio de Ambiente, Vivienda y Desarrollo Territorial, República de Colombia, 2007.

[10] J. Pérez, S. Martín, C. Pinto, B. Cordero, Determination of trihalomethanes in water samples: a review, Anal. Chim. Acta 629 (1–2) (2008) 6–23, https://doi.org/10.1016/j.aca.2008.09.042.

[11] S. Richardson, M. Plewa, E. Wagner, R. Schoeny, D. Demarini, Occurrence, genotoxicity, and carcinogenicity of regulated and emerging disinfection by-products in drinking water: a review and roadmap for research, Mutat. Res./Rev. Mutat. Res. 636 (1–3) (2007) 178–242, https://doi.org/10.1016/j.mrrev.2007.09.001.

[12] S. Krasner, H. Weinberg, S. Richardson, S. Pastor, R. Chinn, M. Sclimenti, G. Onstad, A. Thruston, Occurrence of a new generation of disinfection byproducts, Environ. Sci. Technol. 40 (23) (2006) 7175–7185, https://doi.org/10.1021/es060353j.

[13] Z. Mohd, H. Abu, S. Sheikh, An overview of the technology used to remove trihalomethane (THM), trihalomethane precursors, and trihalomethane formation potential (THMFP) from water and wastewater, J. Ind. Eng. Chem. 57 (2018) 1–14, https://doi.org/10.1016/j.jiec.2017.08.022.

[14] M. Ullberg, E. Lavonen, S. Köhler, O. Golovko, K. Wiberg, Pilot-scale removal of organic micropollutants and natural organic matter from drinking water using ozonation followed by granular activated carbon, Environ. Sci. Water Res. Technol. 7 (3) (2021) 535–548, https://doi.org/10.1039/d0ew00933d.

[15] J. Li, Y. Song, J. Jiang, T. Yang, Y. Cao, Oxidative treatment of NOM by selective oxidants in drinking water treatment and its impact on DBP formation in postchlorination, Sci. Total Environ. 858 (2023) 159908, https://doi.org/10.1016/j.scitotenv.2022.159908.

[16] Y. Zhang, H. Wang, Y. Li, B. Wang, J. Huang, S. Deng, G. Yu, Y. Wang, Removal of micropollutants by an electrochemically driven UV/chlorine process for decentralized water treatment, Water Res. 183 (2020) 116115, https://doi.org/10.1016/j.watres.2020.116115.

[17] A. García, C. Portilla, R. Torres, A. Hidalgo, L. Galeano, Catalytic wet peroxide oxidation of natural organic matter to enhance the treatment of real surface water at urban and rural drinking water plants, J. Water Process Eng. 42 (2021) 102136, https://doi.org/10.1016/j.jwpe.2021.102136.

[18] M. Sillanpaa, M. Ncibi, A. Matilainen, Advanced oxidation processes for the removal of natural organic matter from drinking water sources: a comprehensive review, J. Environ. Manag. 208 (2018) 56–76, https://doi.org/10.1016/j.jenvman.2017.12.009.

[19] L. Galeano, P. Bravo, C. Luna, M. Vicente, A. Gil, Removal of natural organic matter for drinking water production by Al/Fe-PILC-catalyzed wet peroxide oxidation: effect of the catalyst preparation from concentrated precursors, Appl. Catal. B Environ. 111–112 (2012) 527–535, https://doi.org/10.1016/j.apcatb.2011.11.004.

[20] L. Galeano, A. Gil, M. Vicente, Effect of the atomic active metal ratio in Al/Fe, Al/Cu- and Al/(Fe–Cu)-intercalating solutions on the hysicochemical properties and catalytic activity of pillared clays in the CWPO of methyl orange, Appl. Catal. B Environ. 100 (1–2) (2010) 271–281, https://doi.org/10.1016/j.apcatb.2010.08.003.

[21] L. Galeano, M. Vicente, A. Gil, Catalytic degradation of organic pollutants in aqueous streams by mixed Al/M-pillared clays (M = Fe, Cu, Mn), Catal. Rev. Sci. Eng. 56 (2014) 239–287, https://doi.org/10.1080/01614940.2014.904182.

[22] P. Brussino, M. Gross, M. Ulla, E. Banús, Copper and iron-based monolithic catalysts for phenol Catalytic Wet Peroxide Oxidation (CWPO): support and iron effects on the catalytic performance, J. Environ. Chem. Eng. 11 (5) (2023) 110858, https://doi.org/10.1016/j.jece.2023.110858.

[23] Y. Yang, M. Liu, X. You, Y. Li, H. Lin, J. Chen, A novel bimetallic Fe-Cu-CNT catalyst for effective catalytic wet peroxide oxidation: reaction optimization and mechanism investigation, Chem. Eng. J. 479 (2024) 147320, https://doi.org/10.1016/j.cej.2023.147320.

[24] C. Portilla, A. García, F. Dappozze, Ch. Guillard, L. Galeano, Visible-light enhanced catalytic wet peroxide oxidation of natural organic matter in the presence of Al/Fe-pillared clay, Catalysts 11 (5) (2021) 637, https://doi.org/10.3390/catal11050637.

[25] G. Pinchao, L. Ortiz, L. Galeano, A. Hidalgo, J. Ramírez, Optimized CWPO oxidation of natural organic matter in continuous fixed bed reactor catalyzed by an extruded Al/Fe-PILC clay catalyst, J. Environ. Chem. Eng. 9 (1) (2021) 104634, https://doi.org/10.1016/j.jece.2020.104634.

[26] M. Kumari, S. Gupta, A novel process of adsorption cum enhanced coagulation-flocculation spiked with magnetic nanoadsorbents for the removal of aromatic and hydrophobic fraction of natural organic matter along with turbidity from drinking water, J. Clean. Prod. 244 (2020) 118899, https://doi.org/10.1016/j.jclepro.2019.118899.

[27] J. Leenheer, J. Croué, Characterizing dissolved aquatic organic matter, Environ. Sci. Technol. 37 (1) (2003) 18A–26A, https://doi.org/10.1021/es032333c.

[28] B. Liu, J. Yin, J. Wu, X. Cheng, K. Yang, G. Li, Z. Shi, Effect of UV/ClO$_2$ pretreatment on controlling ultrafiltration membrane fouling of different natural organic matter (NOM) fractions, J. Water Process Eng. 49 (2022) 103156, https://doi.org/10.1016/j.jwpe.2022.103156.

[29] L.C. Hua, S.J. Chao, K. Huang, C. Huang, Characteristics of low and high SUVA precursors: relationships among molecular weight, fluorescence, and chemical composition with DBP formation, Sci. Total Environ. 727 (2020) 138638, https://doi.org/10.1016/j.scitotenv.2020.138638.

[30] R. Yu, R. Yang, L. Tian, X. Li, C. Liu, T. Sun, H. Chang, Z. Zhou, Revealing the membrane fouling behavior and interfacial interaction mechanism in a combined visible light photocatalysis-ultrafiltration system for advanced purification of NOM, J. Water Process Eng. 57 (2024) 104723, https://doi.org/10.1016/j.jwpe.2023.104723.

[31] M. Kennedy, H. Chun, V. Yangali, B. Heijman, J. Schippers, Natural organic matter (NOM) fouling of ultrafiltration membranes: fractionation of NOM in surface water and characterisation by LC-OCD, Desalination 178 (1–3) (2005) 73–83, https://doi.org/10.1016/j.desal.2005.02.004.

[32] A. Tubic, J. Agbaba, B. Dalmacija, J. Molnar, S. Maletic, M. Watson, S. Perovic, Insight into changes during coagulation in NOM reactivity for trihalomethanes and haloacetic acids formation, J. Environ. Manag. 118 (2013) 153–160, https://doi.org/10.1016/j.jenvman.2012.11.046.

[33] N. Karapinar, V. Uyak, S. Soylu, T. Topal, Seasonal variations of NOM composition and their reactivity in a low humic water, Prog. Sustain. Energy 33 (3) (2013) 962–971, https://doi.org/10.1002/ep.11878.

[34] C. Li, D. Wang, X. Xiong, Z. Wang, Formation of known and unknown disinfection by-products from natural organic matter fractions during chlorination, chloramination, and ozonation, Sci. Total Environ. 587–588 (2017) 177–184, https://doi.org/10.1016/j.scitotenv.2017.02.108.

[35] K. Berthi, G. Peñuela, Evaluation of a dead-end ultrafiltration membrane for the removal of organic matter from a water reservoir in Colombia, Environ. Res. Eng. Manage. 72 (3) (2016) 27–36, https://doi.org/10.5755/j01.erem.72.3.12906.

[36] Y. Mao, D. Guo, W. Yao, X. Wang, H. Yang, Y. Xie, S. Komarneni, G. Yu, Y. Wang, Effects of conventional ozonation and electro-peroxone pretreatment of surface water on disinfection by-product formation during subsequent chlorination, Water Res. 130 (2018) 322–332, https://doi.org/10.1016/j.watres.2017.12.019.

[37] B. Mayer, D. Ryan, in: A. Gil, L. Galeano, M. Vicente (Eds.), Applications of Advanced Oxidation Processes (AOPs) in Drinking Water Treatment, Springer, Berlin, Heidelberg, 2019, pp. 345–386, https://doi.org/10.1007/978-3-319-76882-3.

[38] J. Xiao, Q. Yue, B. Gao, Y. Sun, J. Kong, Y. Gao, Q. Li, Y. Wang, Performance of activated carbon/nanoscale zero-valent iron for removal of trihalomethanes (THMs) at infinitesimal concentration in drinking water, Chem. Eng. J. 253 (2014) 63–72, https://doi.org/10.1016/j.cej.2014.05.030.

[39] X. Zhang, J. Talley, B. Boggess, G. Ding, D. Birdsell, Fast selective detection of polar brominated disinfection byproducts in drinking water using precursor ion scans, Environ. Sci. Technol. 42 (17) (2008) 6598–6603, https://doi.org/10.1021/es800855b.

[40] A. García, R. Torres, L. Galeano, M. Vicente, A. Gil, Separation and characterization of NOM intermediates along AOP oxidation, in: A. Gil, L. Galeano, M. Vicente (Eds.), Applications of Advanced Oxidation Processes (AOPs) in Drinking Water Treatment, Springer International Publishing, Berlin, 2019, pp. 99–132, https://doi.org/10.1007/978-3-319-76882-3.

[41] D. Myat, M. Mergen, O. Zhao, M. Stewart, J. Orbell, S. Gray, Characterisation of organic matter in IX and PACl treated wastewater in relation to the fouling of a hydrophobic polypropylene membrane, Water Res. 46 (16) (2012) 5151–5164, https://doi.org/10.1016/j.watres.2012.06.054.

[42] J. Swietlik, E. Sikorska, Characterization of natural organic matter fractions by high pressure size-exclusion chromatography, specific UV absorbance and total luminescence spectroscopy, Pol. J. Environ. Stud. 15 (1) (2005) 145–153.

[43] A. Ordonez, D. Revelo, A. Garcia, A. Hidalgo, L. Galeano, MS2 coliphage inactivation by Al/Fe PILC-activated catalytic wet peroxide oxidation: multiresponse statistical optimization, Heliyon 5 (6) (2019) e01892, https://doi.org/10.1016/j.heliyon.2019.e01892.

[44] S. Liu, M. Lim, R. Fabris, C. Chow, M. Drikas, R. Amal, TiO$_2$ photocatalysis of natural organic matter in surface water: impact on trihalomethane and haloacetic acid formation potential, Environ. Sci. Technol. 42 (16) (2008) 6218–6223, https://doi.org/10.1021/es800887s.

[45] APHA-AWWA-WEF, Standard Methods for the Examination of Water and Wastewater, American Public Health Association, American Water Works Association, Water Environment Federation, Washington, DC, 2017.

[46] L. Yang, Q. She, M. Wan, R. Wang, V. Chang, C. Tang, Removal of haloacetic acids from swimming pool water by reverse osmosis and nanofiltration, Water Res. 116 (2017) 116–125, https://doi.org/10.1016/j.watres.2017.03.025.

[47] C. Zhao, Y. Fujii, J. Yan, K. Harada, A. Koizumi, Pentafluorobenzyl esterification of haloacetic acids in tap water for simple and sensitive analysis by gas chromatography/mass spectrometry with negative chemical ionization, Chemosphere 119 (2015) 711–718, https://doi.org/10.1016/j.chemosphere.2014.07.048.

[48] Z. Liu, Z. Wei, A. Li, H. Yang, Enhanced coagulation of low-turbidity micro-polluted surface water: properties and optimization, J. Environ. Manag. 233 (2019) 739–747, https://doi.org/10.1016/j.jenvman.2018.08.101.

[49] Y. Zhao, F. Xiao, D. Wang, M. Yan, Z. Bi, Disinfection byproduct precursor removal by enhanced coagulation and their distribution in chemical fractions, J. Environ. Sci. 25 (11) (2013) 2207–2213, https://doi.org/10.1016/S1001-0742(12)60286-1.

[50] J. Sanchis, A. Jaen, P. Gago, E. Munthali, M. Farre, Characterization of organic matter by HRMS in surface waters: effects of chlorination on molecular fingerprints and correlation with DBP formation potential, Water Res. 176 (2020) 115743, https://doi.org/10.1016/j.watres.2020.115743.

[51] H. Hong, X. Yan, X. Qin, H. Sun, H. Lin, J. Chen, Y. Liang, Bromine incorporation into five DBP classes upon chlorination of water with extremely low SUVA values, Sci. Total Environ. 590–591 (2017) 720–728, https://doi.org/10.1016/j.scitotenv.2017.03.032.

[52] C. Huang, C. Chen, G. Wang, Temperature dependence of characteristics of organic precursors, bromide, and disinfection byproduct formation, Sci. Total Environ. 662 (2019) 746–754, https://doi.org/10.1016/j.scitotenv.2019.01.239.

[53] M. Sillanpää, A. Matilainen, in: M. Sillanpää (Ed.), Natural Organic Matter in Water. Characterization and Treatment Methods, Butterworth-Heinemann, USA, 2015, pp. 55–80.

[54] Z. Gao, Y. Lin, B. Xu, Y. Xia, C. Hu, T. Zhang, H. Qian, T. Cao, N. Gao, Effect of bromide and iodide on halogenated by-product formation from different organic precursors during UV/chlorine processes, Water Res. 182 (2020) 116035, https://doi.org/10.1016/j.watres.2020.116035.

[55] H. Wang, Y. Zhu, C. Hu, X. Hu, Treatment of NOM fractions of reservoir sediments: effect of UV and chlorination on formation of DBPs, Sep. Purif. Technol. 154 (2015) 228–235, https://doi.org/10.1016/j.seppur.2015.09.031.

[56] S. Chowdhury, P. Champagne, P. James McLellan, Investigating effects of bromide ions on trihalomethanes and developing model for predicting bromodichloromethane in drinking water, Water Res. 44 (7) (2010) 2349–2359, https://doi.org/10.1016/j.watres.2009.12.042.

[57] Y. Chen, T. Lin, W. Chen, Enhanced removal of organic matter and typical disinfection byproduct precursors in combined iron-carbon micro electrolysis-UBAF process for drinking water pre-treatment, J. Environ. Sci. (China) 78 (2019) 315–327, https://doi.org/10.1016/j.jes.2018.11.010.

[58] T. Bond, E. Goslan, B. Jefferson, F. Roddick, L. Fan, S. Parsons, Chemical and biological oxidation of NOM surrogates and effect on HAA formation, Water Res. 43 (10) (2009) 2615–2622, https://doi.org/10.1016/j.watres.2009.03.036.